Infrared-reflectivity study of ZrO_2-HfO_2 solid solutions

T. Hirata
National Research Institute for Metals, 2-3-12, Nakameguro, Meguro-ku, Tokyo 153, Japan
(Received 28 February 1994)

Infrared-reflectance spectra of the solid solutions $Zr_{1-x}Hf_xO_2$ ($0 \le x \le 1$) have been measured at room temperature in the frequency region 50–4000 cm^{-1} by Fourier-transform infrared spectroscopy in order to study the composition effect on the vibrational properties of $Zr_{1-x}Hf_xO_2$. At most, twelve infrared-active modes of $5A_u$ and $7B_u$ symmetry were identified in the reflectance spectra of $Zr_{1-x}Hf_xO_2$. The spectra of $Zr_{1-x}Hf_xO_2$ varied systematically with x, with changes in the frequency, linewidth, and intensity of these modes. Particularly, the B_u modes at 585 and 606 cm^{-1} for ZrO_2 considerably stiffened in a nonlinear way, indicating a pronounced stiffening around $x=0.8$ as x increases. It was found that the lattice parameters a, b, and c of $Zr_{1-x}Hf_xO_2$ decrease linearly with x whereas β initially increases up to $x=0.6$ and then decreases towards that of the end member HfO_2. Hence, it was concluded that the stiffening of all other modes except a B_u mode is associated with the bond reinforcement evidenced by the reduced cell volume of $Zr_{1-x}Hf_xO_2$ as the Hf^{4+} ions of smaller radius are substituted for the Zr^{4+} ions. It was also concluded that the anomalous feature around $x=0.8$ in the frequency, linewidth, and intensity of the modes as a function of x can be reconciled with two-mode behavior, which has been characterized by discontinuities at either $x=0.6$ or 0.3 in the x dependence of seven Raman mode frequencies for $Zr_xHf_{1-x}O_2$ [C. Carlone, Phys. Rev. B **45**, 2079 (1992)].

I. INTRODUCTION

Zirconia (ZrO_2) has chemical and physical properties similar to hafnia (HfO_2). Both oxides crystallize in a low-symmetry crystal structure (monoclinic) with four formula units per unit cell (space group C_{2h}^5; $P2_1/c$). The lattice parameters of ZrO_2 are $a=5.150$ Å, $b=5.211$ Å, $c=5.317$ Å, and $\beta=99.23°$,[1] whereas the unit cell of HfO_2 is slightly modified: $a=5.1170$ Å, $b=5.1754$ Å, $c=5.2915$ Å, and $\beta=99.21°$.[2] The same crystal structure and similar properties of both oxides mean that they can form a series of solid solutions, $Zr_{1-x}Hf_xO_2$, over a wide concentration range ($0 \le x \le 1$) in the ZrO_2-HfO_2 system.

A Raman spectroscopic study of the solid solutions $Zr_{1-x}Hf_xO_2$ has been done in the context of the composition effect on optical modes of mixed crystals.[3] Krebs and Condrate[4] have found that some Raman modes of A_g or B_g symmetry in the high-frequency region shift almost linearly with x from one end member to another, suggesting one-mode behavior. On the other hand, Carlone[5] has found that the Raman spectra of $Zr_{1-x}Hf_xO_2$ exhibit both one- and two-mode behavior depending on the optical modes; the two-mode behavior is characterized by discontinuities at either $x=0.3$ or $x=0.6$ in the x dependence of seven Raman mode frequencies for $Zr_xHf_{1-x}O_2$.

A group theoretical analysis yields the following irreducible representations of optical modes at the wave vector $k=0$ for the monoclinic structure of ZrO_2 and HfO_2:[6,7]

$$\Gamma_{\text{vib}}=9A_g(\text{R})+9B_g(\text{R})+8A_u(\text{IR})+7B_u(\text{IR}) .$$

The Raman spectroscopic study[5] on the mode behavior of $Zr_xHf_{1-x}O_2$ was done by observing and assigning the Raman-active modes $9A_g$ and $9B_g$. As there exist 15 infrared-active modes ($8A_u+7B_u$), it is also possible to look into the mode behavior of $Zr_{1-x}Hf_xO_2$ by infrared spectroscopy. While Krebs and Condrate[4] have stated that the infrared bands of $Zr_{1-x}Hf_xO_2$ shift as x increases, the infrared spectra were not provided, nor an analysis because of the infrared bands being broad.

The present investigation concerns the effect of composition on vibrational properties of the solid solutions $Zr_{1-x}Hf_xO_2$ by infrared spectroscopy. In addition, the unit-cell dimensions of $Zr_{1-x}Hf_xO_2$, which have not been reported to the author's knowledge, were determined as well. The unit-cell dimensions are associated with cation-anion bond lengths, such that the bond-length changes greatly affect the A_u and B_u modes that correspond to the atomic displacements parallel to the c axis and in the ab plane, respectively. Thus, it is essential to know how the lattice parameters of $Zr_{1-x}Hf_xO_2$ change as a function of x to understand the composition effect on the vibrational properties of $Zr_{1-x}Hf_xO_2$.

II. EXPERIMENTAL

The solid solutions $Zr_{1-x}Hf_xO_2$($0 \le x \le 1$) were prepared by the solid-state reaction method rather than starting with the mixed hydroxide of ZrO_2-HfO_2 solid solutions.[4] Appropriate amounts of ZrO_2 (99.9%) and HfO_2 (99.9%) in order to change the value of x by 0.1 were thoroughly mixed and formed into pellets (10 mm in diameter and ~1 mm in thickness). These pellets were sintered at 800 °C for 24 h, and then reground, pelletized, and finally sintered at 1450 °C for 7 h.

X-ray diffraction (XRD) with Cu $K\alpha$ radiation confirmed a series of solid solutions $Zr_{1-x}Hf_xO_2$ over the entire concentration range ($0 \le x \le 1$). Lattice parame-

ters were determined by using a computer program with the reflections in the range $2\theta=10°-80°$ and Si as an internal standard.

Infrared-reflectance spectra of the as-prepared pellets were measured at room temperature by Fourier-transform infrared spectroscopy (model JEOR100), in two different frequency regions, 400–4000 cm^{-1} and 50–600 cm^{-1}, respectively. Resolution was 4 cm^{-1} in the midinfrared region and 2 cm^{-1} in the far-infrared one. Either beam splitter, KBr or Mylar, was used to measure infrared-reflectance spectra in each frequency region; a TGS (triglycine sulfate) detector was used. A mirror of an evaporated thin film of aluminum was used to measure the reference spectrum in each frequency region, and the infrared-reflectance spectra of $Zr_{1-x}Hf_xO_2$ are represented as the intensity ratios of the measured spectra with respect to the reference spectrum.

III. RESULTS

A. Lattice parameters

Powder XRD indicated no formation of any ternary compound(s), confirming a series of solid solutions $Zr_{1-x}Hf_xO_2$ over the entire concentration range $(0\leq x\leq 1)$. The lattice parameters and the unit-cell volume of $Zr_{1-x}Hf_xO_2$ are shown as a function of x in Fig. 1. The lattice parameters a, b, and c decrease linearly with x conforming to Vegard's law, whereas β initially increases up to $x=0.6$ and then decreases toward that of the end member HfO_2 as x increases. The lattice parameters a, b, and c of ZrO_2 and HfO_2 ($a=5.1501$ Å, $b=5.2109$ Å, $c=5.3157$ Å, and $\beta=99.268°$ for ZrO_2; $a=5.1197$ Å, $b=5.1781$ Å, $c=5.2918$ Å, and $\beta=99.278°$ for HfO_2) are comparable to the literature data[1,2] although the β's are slightly larger than those in Refs. 1 and 2. The concentration dependence of β causes a deviation from linearity above $x=0.6$ in the unit-cell volume ($V=abc\sin\beta$) vs x plot.

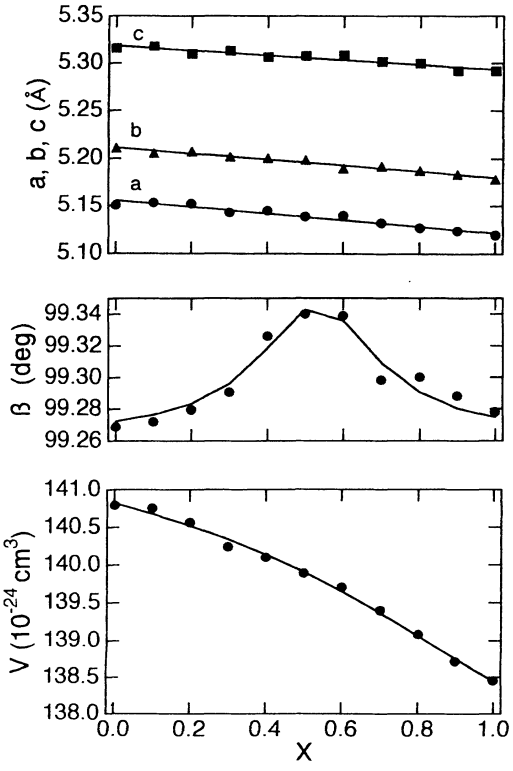

FIG. 1. Lattice parameters a, b, c, and β as a function of x for $Zr_{1-x}Hf_xO_2$; the unit-cell volume V ($V=abc\sin\beta$) is plotted as well.

A neutron-diffraction study[8] has indicated that the lattice parameters a, b, and c of monoclinic ZrO_2 decrease whereas β increases while cooling from 1250 to 300 K; these lattice-parameter changes are similar to those up to $x=0.6$ for $Zr_{1-x}Hf_xO_2$. Hence, the lattice contraction while cooling and the substitution for Zr by Hf of smaller radius may affect the lattice parameters of ZrO_2 similarly. The substitution of Hf for Zr above $x=0.6$ leads to a decrease in β.

B. Infrared-reflectance spectra

The infrared-reflectance spectra of $Zr_{1-x}Hf_xO_2$, ZrO_2, and HfO_2 for reference are shown in Fig. 2; note that each spectrum is offset vertically for clarity and displayed in two frequency regions that partly overlap. The transmission spectrum of monoclinic ZrO_2 (Ref. 9) can be compared with the infrared-reflectance spectrum of ZrO_2 in the present work. However, we would stress that our infrared-reflectance spectrum is more informative concerning the infrared-active modes. The frequencies and symmetries of infrared modes for monoclinic ZrO_2 at 300 K are summarized as follows:[10] 104 cm^{-1} (A_u), 180 cm^{-1} (A_u), 192 cm^{-1} (A_u), 233 cm^{-1} (A_u), 270 cm^{-1} (A_u), 360 cm^{-1} (B_u), 373 cm^{-1} (B_u), 415 cm^{-1} (A_u), 443 cm^{-1} (A_u), 515 cm^{-1} ($2B_u$), 620 cm^{-1} ($2B_u$), and 740 cm^{-1} (A_u and B_u). Among these infrared modes, twelve infrared modes of $5A_u$ and $7B_u$ can be identified approximately at 220 cm^{-1} (A_u), 250 cm^{-1} (A_u), 330 cm^{-1} (B_u), 370 cm^{-1} (B_u), 420 cm^{-1} (A_u), 440 cm^{-1} (A_u), 520 cm^{-1} ($2B_u$), 600 cm^{-1} ($2B_u$), and 740 cm^{-1} (A_u and B_u) in the infrared-reflectance spectrum of ZrO_2. No A_u modes at 104, 180, and 192 cm^{-1} are apparent in Fig. 2. We can notice that the A_u mode at 443 cm^{-1} for ZrO_2 is apparent as a shoulder and becomes invisible as the A_u mode at 420 cm^{-1} increases in intensity with x. The B_u mode at 330 cm^{-1} also appears as a shoulderlike feature, which becomes pronounced with x as noted for HfO_2. It is noteworthy that the infrared-reflectance spectra of $Zr_{1-x}Hf_xO_2$ vary systematically with x, changing the position, linewidth, and intensity of these infrared modes. It is particularly noticeable that the infrared mode at 600 cm^{-1} ($2B_u$) stiffens considerably, changing in intensity and/or linewidth as x increases.

C. Analysis

In the present work, no infrared-reflectance spectra consisting of the $5A_u+7B_u$ modes have been analyzed

based on the classical dispersion theory together with a Kramers-Kronig analysis,[11,12] whereby we can obtain the dispersion parameters such as resonance frequency, damping factor, and oscillator strength; we may expect that these parameters change depending on x. Instead, curve-fitting procedures have been performed to assess the exact position as well as the linewidth of each infrared mode, using a computer program installed with our infrared spectrometer.

The position, height, and width were all varied as fitting parameters so as to obtain the best fit to the experimentally observed infrared bands. It turned out that the best fit to the observed ir bands can be achieved with two Gaussian curves.

A curve fitting to the infrared mode ($2B_u$) at 600 cm^{-1} for $Zr_{1-x}Hf_xO_2$ ($x=0.7$) is exemplified in Fig. 3. The ir mode frequencies thus determined are plotted as a function of x for $Zr_{1-x}Hf_xO_2$ in Fig. 4. It is reasonable to decompose the infrared modes at 600 cm^{-1} ($2B_u$), 515 cm^{-1} ($2B_u$), 330–370 cm^{-1} (B_u), 410–445 cm^{-1} (A_u), and 740 cm^{-1} (A_u and B_u) into two parts because these infrared modes are doubly degenerate or overlapping each other. In fact, the curve-fitting procedures were successful with two Gaussian curves for these infrared modes. No successful fitting was possible with a single Gaussian curve for the A_u mode at 220 cm^{-1}; at least two Gaussian curves were necessary to attain an acceptable fit to the experiment, so that the peak frequency of the synthesis of two decomposed curves is adopted for this infrared mode. For a similar reason, the peak frequency is adopted for the A_u mode at 250 cm^{-1}.

We should notice the following. All the identified ir modes would stiffen with x, except the B_u mode at 355 cm^{-1} which slightly softens with x. The softening of this B_u mode with x may be seen by a subtle downshift of the peak at about 350 cm^{-1} with x (see Fig. 2). It is of particular interest that the B_u modes at 585 and 606 cm^{-1} for ZrO_2 stiffen considerably in a nonlinear way as x increases, indicating a pronounced stiffening around $x=0.8$. This significant stiffening tendency around $x=0.8$ can be observed in the x dependence of the other A_u or B_u modes, as shown in Fig. 3.

Each mode obtained by decomposing the infrared mode ($2B_u$) at 600 cm^{-1}, exhibits an x dependence of the linewidth as shown in Fig. 5 and reveals an anomalous feature around $x=0.8$. On the other hand, the integrat-

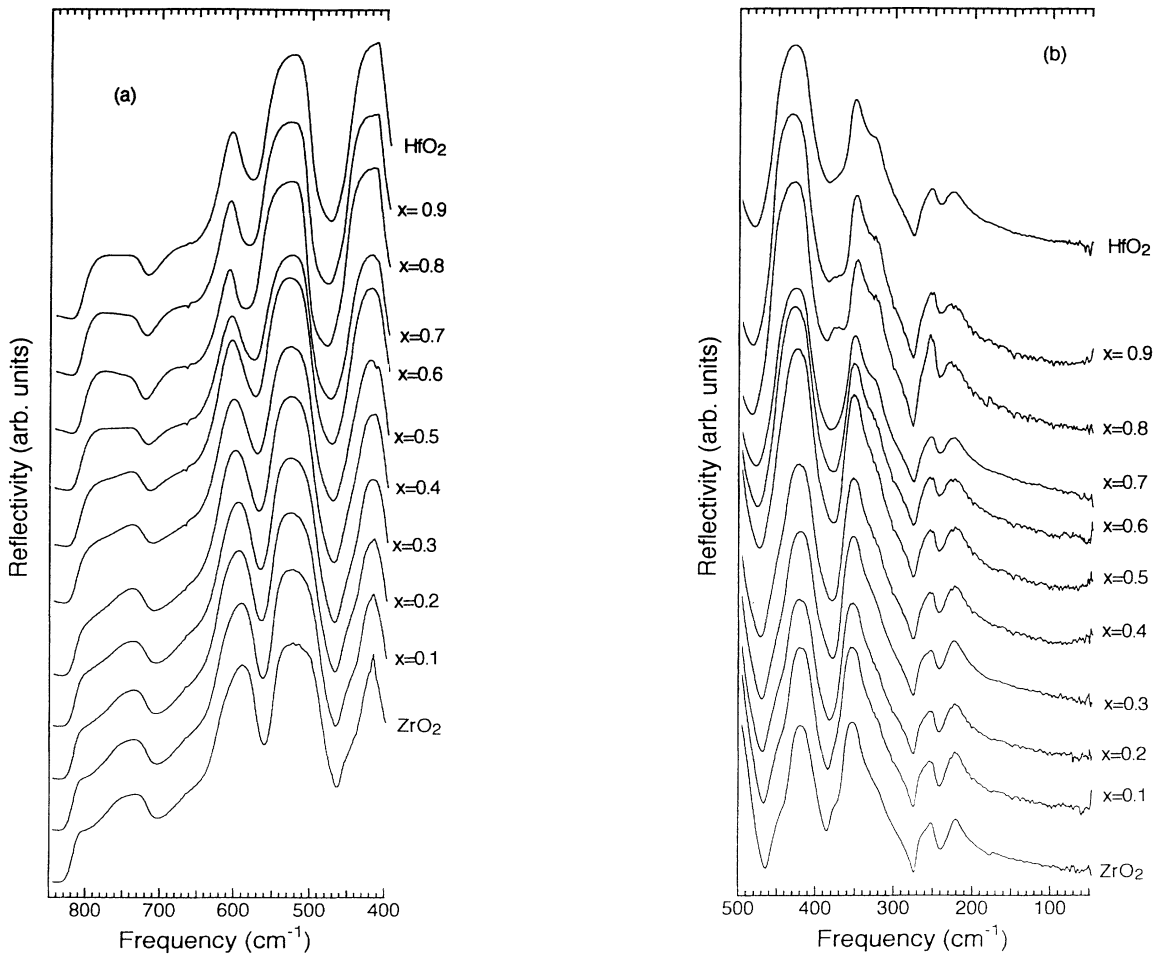

FIG. 2. Infrared-reflectance spectra of $Zr_{1-x}Hf_xO_2$ in two frequency regions that partly overlap: 400–850 cm^{-1} (a) and 50–500 cm^{-1} (b). Each spectrum is offset vertically for clarity.

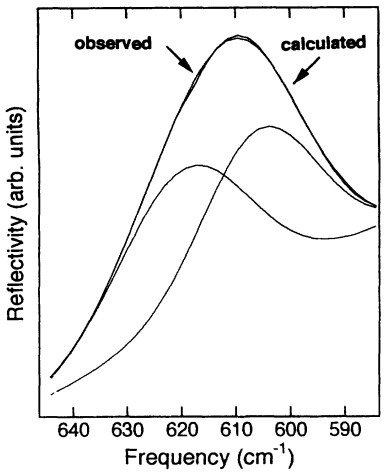

FIG. 3. Curve fitting to the infrared mode ($2B_u$) at 600 cm^{-1} for $Zr_{1-x}Hf_xO_2$ ($x=0.7$) with two Gaussian curves.

ed intensity of the infrared mode at 600 cm^{-1} ($2B_u$) decreases nonlinearly with x, whereas the two A_u modes over 400–600 cm^{-1} increase overall as x increases (Fig. 6). It is interesting to note that the A_u and B_u modes change in intensity in an opposite way with respect to x, and that the anomalous feature around $x=0.8$ is manifested even in the x dependence of the intensity.

IV. DISCUSSION

First, a comment should be made concerning the mode stiffening, where all the identified ir modes except the B_u mode at 355 cm^{-1} increase in frequency with x. The A_u and B_u modes correspond to the atomic displacements parallel to the c axis and in the ab plane, respectively. Consequently, we can conclude that the observed mode stiffening is associated with the reinforcement of bonds responsible for the atomic displacements, which is evidenced by the decrease in the lattice parameters a, b, and c with increasing x in $Zr_{1-x}Hf_xO_2$. In view of the bond

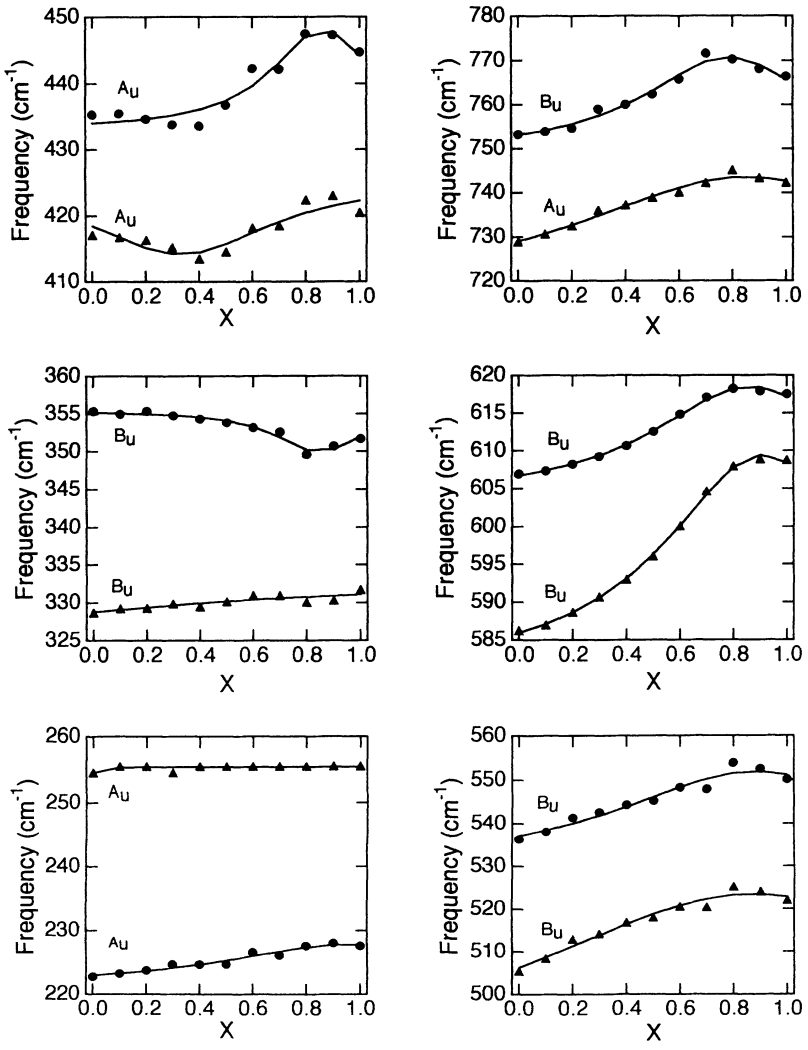

FIG. 4. The ir mode frequencies as a function of x for $Zr_{1-x}Hf_xO_2$; note that the lines connecting the frequencies are only for guiding the eye.

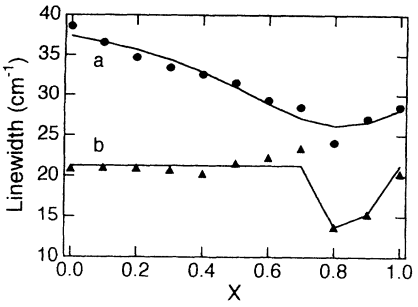

FIG. 5. Linewidths of each mode obtained by decomposing the infrared mode ($2B_u$) at 600 cm^{-1} as a function of x for $Zr_{1-x}Hf_xO_2$. Curve a, for the high-frequency mode; curve b, for the low-frequency mode. The lines are only a guide to the eye.

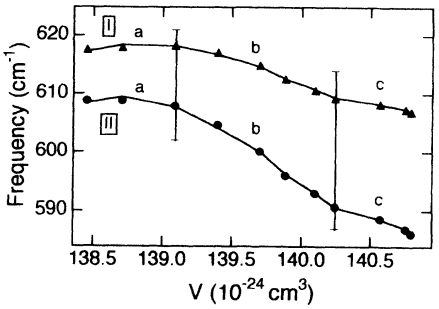

FIG. 7. Relationship between the unit-cell volume V and the mode frequency obtained by decomposing the infrared mode at 600 cm^{-1} ($2B_u$) for $Zr_{1-x}Hf_xO_2$, I, for the high-frequency mode, and II, for the lower-frequency mode.

reinforcement, the x dependence for the B_u mode at 355 cm^{-1} is exceptional; no explanation can be found for this, but it is interesting that this mode also behaves anomalously around $x=0.8$, i.e., yielding a minimum in the x dependence of frequency.

We could find a relation between the unit-cell volume V and the mode frequency obtained by decomposing the mode ($2B_u$) at 600 cm^{-1} for $Zr_{1-x}Hf_xO_2$ as shown in Fig. 7. The observed relation (nonlinear) contradicts a linear relationship between the Sb-O bond-stretching frequency and the unit-cell volume of different $L_3Sb_5O_{12}$ oxides (L = Pr, Nd, Sm, etc.).[13]

This nonlinear relation between V and the mode frequency implies that bond reinforcement does not increase linearly as a function of x in $Zr_{1-x}Hf_xO_2$. Actually, both curves of Fig. 7 can be divided into three regions; the substitution effect on the bond reinforcement is relatively small and still under the control of ZrO_2 in the region c, but it becomes pronounced in the region b, and saturates in the region a near the other end member HfO_2. The reduced unit-cell volume relevant to the bond reinforcement is explained based on the smaller ionic radius of Hf^{4+} (0.78 Å) than Zr^{4+} (0.79 Å),[14] as the Hf ions are substituted for the Zr ions in $Zr_{1-x}Hf_xO_2$.

Secondly, we pay attention to the anomalous feature

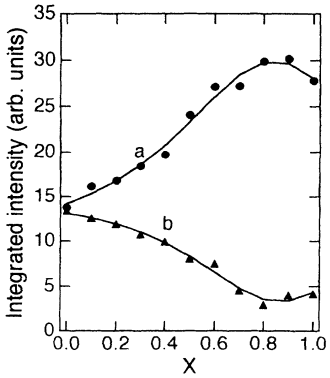

FIG. 6. Integrated intensities of the two A_u modes over 400–460 cm^{-1} (curve a) and the $2B_u$ modes at 600 cm^{-1} (curve b) as a function of x for $Zr_{1-x}Hf_xO_2$.

around $x=0.8$ in the x dependence of frequency, integrated intensity, and linewidth of the modes. At first, it was thought that the samples with high x might contain inhomogeneities. To resolve this problem, we reground the samples with $x=0.7$, 0.8, and 0.9, and we repeated infrared-reflectivity measurements after forming pellets under the same conditions as before. These samples reproduced the anomalous feature in question around $x=0.8$. Hence we can conclude that the observed anomalous feature around $x=0.8$ is inherent in the x dependence of frequency, intensity, and linewidth of the modes for $Zr_{1-x}Hf_xO_2$.

A plausible explanation is that the ZrO_2-HfO_2 solid solutions exhibit two-mode behavior as pointed out by Carlone.[5] He has found that the x dependence of seven Raman mode frequencies is characterized by discontinuities at either $x=0.6$ or $x=0.3$ in $Zr_xHf_{1-x}O_2$. It is of particular interest that these x values are close to the x's ($x=0.3$ and $x=0.8$) at the borderline between each region in Fig. 7; note that Carlone[5] has chosen the x's approximately ($x=0$, 0.1, 0.25, 0.5, 0.75, 0.9, and 1.0) in $Zr_xHf_{1-x}O_2$, which makes a difference in comparison with the present work.

In the random-element-isodisplacement (REI) model,[15–19] it is assumed that the three force constants $f_{ij}(x)$ in a mixed crystal $AB_{1-x}C_x$ ($ij=AB, AC, BC$) have the same compositional dependence such that $f_{ij}(x)=f_{ij}(0)[1+\Theta x]$, where $f_{ij}(0)$ is the force constant at $x=0$ and Θ is a constant which describes the effect of lattice-parameter change on the force constants. When analyzing long-wave optical phonons in mixed crystals based on the REI model,[12,18,20] the constant Θ was allowed to depend on composition. Even so, it seems unlikely that the nonlinear x dependence of frequency as well as the significant stiffening around $x=0.8$ can be reproduced starting with $\nu(x)=[f_{ij}(x)/\mu(x)]^{1/2}$, where $\nu(x)$ is the x dependence of the frequency, and $\mu(x)$ is the reduced mass given by $\mu^{-1}(x)=(1-x)/M_{Zr}+x/M_{Hf}$ for $Zr_{1-x}Hf_xO_2$ with M_{Zr} and M_{Hf} being the masses of Zr and Hf atoms, respectively.

Besides, the lattice parameters a, b, and c decrease linearly with x whereas β increases up to $x=0.6$ and then decreases with x for $Zr_{1-x}Hf_xO_2$. This change in β contradicts the case for $Zr_{1-x}Hf_xS_3$ (Ref. 21) with the same

structure as $Zr_{1-x}Hf_xO_2$, where β increases linearly over the entire range of x ($0 \leq x \leq 1$). We do not know how this change of β should be adjusted to the linear dependence of force constants on the lattice parameter in the REI model.[19]

Under these circumstances, we are inclined to conclude that the solid solutions $Zr_{1-x}Hf_xO_2$ exhibit two-mode behavior which is associated with the anomalous feature around $x=0.8$ in the x dependence of frequency, linewidth, and intensity of the modes. Experimentally, however, it is still necessary to examine whether the samples with high x are free of any microscopic inhomogeneities in the distribution of the constituent atoms.

Finally, we note that the observed anomalous feature is manifested in the infrared spectrum of $Zr_{1-x}Hf_xO_2$ with $x=0.8$ *per se*. We can easily notice that the infrared mode ($2B_u$) at 600 cm^{-1} decreases considerably in linewidth and that a small band at 355 cm^{-1} is apparent as well. The position of this small band is equal to that of the A_u mode (≈ 355 cm^{-1}) for ZrO_2, so it does originate in the perturbation due to the substitution of Zr for Hf in HfO_2; this persistent band was observed even in the infrared spectrum of the $x=0.8$ sample that was reground and measured again.

V. CONCLUSIONS

Infrared-reflectance spectra of the solid solutions $Zr_{1-x}Hf_xO_2$ ($0 \leq x \leq 1$) have been measured at room temperature in the frequency region 50–4000 cm^{-1} by Fourier-transform infrared spectroscopy. At most, twelve infrared-active modes of $5B_u$ and $7A_u$ symmetry were identified in the infrared-reflectance spectra of $Zr_{1-x}Hf_xO_2$. The spectra of $Zr_{1-x}Hf_xO_2$ varied systematically with x, with changes in the frequency, linewidth, and intensity of these modes. In particular, the B_u modes at 585 and 606 cm^{-1} for ZrO_2 considerably stiffened in a nonlinear way, indicating a pronounced stiffening around $x=0.8$ as x increases.

X-ray diffraction revealed that the lattice parameters, a, b, and c of $Zr_{1-x}Hf_xO_2$ decrease linearly with x whereas β initially increases up to $x=0.6$ and then decreases with x. Hence, we concluded that the stiffening of the identified ir modes is associated with the bond reinforcement evidenced by the reduced cell volume of $Zr_{1-x}Hf_xO_2$ when the Hf^{4+} ions of smaller radius than Zr^{4+} are substituted for the Zr^{4+} ions.

It is also concluded that the anomalous feature around $x=0.8$ in the x dependence of frequency, linewidth, and intensity of the modes can be reconciled with two-mode behavior, which was characterized by discontinuities at either $x=0.6$ or 0.3 in the x dependence of seven Raman mode frequencies for $Zr_xHf_{1-x}O_2$.[5]

ACKNOWLEDGMENTS

The author greatly thanks H. Doi for powder x-ray diffraction. Thanks are also due to Dr. K. Saito and Dr. K. G. Nakamura for discussions.

[1]C. J. Howard, R. J. Hill, and B. E. Reichert, Acta Crystallogr. Sect. B **44**, 116 (1988).
[2]R. E. Hahn, P. R. Suitch, and J. L. Pentecost, J. Am. Ceram. Soc. **68**, C-285 (1985).
[3]R. J. Elliot and I. P. Ipatova, *Optical Properties of Mixed Crystals* (North-Holland, Amsterdam, 1988).
[4]M. A. Krebs and R. A. Condrate, J. Am. Ceram. Soc. **67**, C-144 (1982).
[5]C. Carlone, Phys. Rev. B **45**, 2079 (1992).
[6]E. Anastassakis, B. Papanicolaou, and I. M. Asher, J. Phys. Chem. Solids **36**, 667 (1975).
[7]V. G. Keramidas and W. B. White, J. Am. Ceram. Soc. **57**, 22 (1974).
[8]H. Boysen, F. Frey, and T. Vogt, Acta Crystallogr. Sect. B **47**, 881 (1991).
[9]C. M. Phillippi and K. S. Mazdiyasni, J. Am. Ceram. Soc. **54**, 254 (1971).
[10]A. Feinberg and C. H. Perry, J. Phys. Chem. Solids **42**, 513 (1980).
[11]M. H. Brodsky, G. Lucovsky, M. F. Chen, and T. S. Plaskett, Phys. Rev. B **2**, 3303 (1970).
[12]G. Lucovsky, K. Y. Cheng, and G. L. Pearson, Phys. Rev. B **12**, 4135 (1975).
[13]I. L. Botto, E. J. Baran, C. Cascales, I. Rasines, and R. Saez Puche, J. Phys. Chem. Solids **52**, 431 (1991).
[14]*Handbook of Chemistry and Physics*, 53rd ed., edited by R. C. Weast (Chemical Rubber, Cleveland, 1972–1973).
[15]Y. S. Chen, W. Shockley, and G. L. Pearson, Phys. Rev. **151**, 648 (1966).
[16]M. Ilegems and G. L. Pearson, Phys. Rev. B **1**, 1576 (1970).
[17]G. Lucovsky, K. Y. Cheng, and G. L. Pearson, Phys. Rev. B **12**, 4135 (1975).
[18]G. Lucovsky, R. D. Burnham, and A. S. Alimonda, Phys. Rev. B **14**, 2503 (1976).
[19]D. L. Peterson, A. Petrou, W. Giriat, A. K. Ramdas, and S. Rodriguez, Phys. Rev. B **33**, 1160 (1986).
[20]P. D. Lao, Yile Guo, G. G. Siu, and S. C. Shen, Phys. Rev. B **48**, 11 701 (1993).
[21]G. Nouvel, A. Zwick, M. A. Renucci, and A. Kjekshus, Phys. Rev. B **32**, 1165 (1985).